Experimental Results of the Novel 1.5-MW-Class 140-GHz Continuous-Wave Gyrotron for the Wendelstein 7-X Stellarator

S. Ponomarenko, H. P. Laqua, K. A. Avramidis, G. Gantenbein, J. Gontard, F. Hollmann, S. Illy, Z. C. Ioannidis, *Member, IEEE*, J. Jelonnek, *Senior Member, IEEE*, J. Jin, S. Kohler, L. Krier, A. Leggieri, F. Legrand, G. Lietaer, C. Lievin, S. Marsen, D. Moseev, F. Noke, T. Rzesnicki, T. Stange, M. Thumm, *Life Fellow, IEEE*, and R. C. Wolf

***Abstract*— In this work, we present the achievements obtained during the commissioning phase of the newly developed 140-GHz continuous-wave tube TH1507U at the gyrotron test stand of the electron-cyclotron resonance heating facility of the Wendelstein 7-X stellarator. The gyrotron is based on the successful 1-MW class industrial TH1507 gyrotron, which operates in the $TE_{28,8}$ mode, and has been optimized for operation in the higher-order $TE_{28,10}$ mode. The 1-ms short-pulse tests confirmed the nominal output power of 1.5 MW. In a long-pulse operating regime, an output power of 1.3 MW with total efficiency 45.9% was demonstrated at pulse lengths of 3 minutes. Different regimes where the beam current is above 50 A demonstrated a saturation of output power at 1.3 MW, that can be explained by the presence of parasitic modes. A parasite-free operation with an output power of 1.2 MW was achieved with pulses up to 580 s in length. The pulse length was limited due to the existing capabilities of the cooling system at the test stand, and is foreseen to be extended in the future.**

***Index Terms*— Gyrotrons, high-power microwave generation, electromagnetic heating, ECRH.**

Received 10 September 2024; revised 9 October 2024; accepted 16 October 2024. Date of publication 21 October 2024; date of current version 26 November 2024. This work was supported by the EUROfusion Consortium, funded by the European Union via the Euratom Research and Training Program—EUROfusion under Grant 101052200. The review of this letter was arranged by Editor N. M. Ryskin. *(Corresponding author: S. Ponomarenko.)*

S. Ponomarenko, H. P. Laqua, F. Hollmann, L. Krier, S. Marsen, D. Moseev, F. Noke, T. Stange, and R. C. Wolf are with the Max Planck Institute for Plasma Physics, 17491 Greifswald, Germany (e-mail: sergiy.ponomarenko@ipp.mpg.de).

K. A. Avramidis is with the Department of Physics, National and Kapodistrian University of Athens, 157 84 Athens, Greece.

G. Gantenbein, S. Illy, J. Jelonnek, J. Jin, T. Rzesnicki, and M. Thumm are with the Institute for Pulsed Power and Microwave Technology, Karlsruhe Institute of Technology, 76131 Karlsruhe, Germany.

J. Gontard, S. Kohler, A. Leggieri, F. Legrand, G. Lietaer, and C. Lievin are with the THALES Microwave and Imaging Sub-Systems, 78141 Vélizy-Villacoublay, France.

Z. C. Ioannidis is with the Department of Aerospace Science and Technology, National and Kapodistrian University of Athens, Euripus Campus, 344 00 Psachna, Greece.

Color versions of one or more figures in this letter are available at https://doi.org/10.1109/LED.2024.3484218.

Digital Object Identifier 10.1109/LED.2024.3484218

I. Introduction

In THE next years, the power available from the electron-cyclotron resonance heating (ECRH) system of the largest experimental stellarator Wendelstein 7-X (W7-X) shall be increased from 8.6 MW to 18 MW to achieve the design values and to demonstrate improved fast ion confinement in the plasma [1], [2]. For this reason, the development of a new 1.5-MW class continuous-wave (CW) gyrotron was initiated within the German Helmholtz Innovation Pool project HIPOWER and is continued in the EUROfusion project [3], [4], [5], [6]. The manufacturing partner for the industrial gyrotrons is Thales. According to the specification, the new design must be compliant with the existing ECRH gyrotron installations at W7-X. In order to retain the existing electron optics and the profile of the magnetic focusing field, the new gyrotron employs an enlarged cavity and nominally operates in the higher-order $TE_{28,10}$ mode in contrast to the $TE_{28,8}$ mode, presently used in the 1-MW-class industrial TH1507 gyrotrons [7], [8]. The larger surface area combined with improved uniform cavity cooling allows the output power to be increased to 1.5 MW without exceeding the critical surface power density of 2 kW/cm^2 in the resonator. The diode electron gun was adapted to run beam currents up to 60 A. Improvements included a new mode converter designed to convert the $TE_{28,10}$ mode to the fundamental Gaussian mode with over 98% efficiency. The last internal gyrotron mirror, M3, has an externally movable suspension for precise Gaussian beam centering at the output window. Furthermore, the beam tunnel between the gun and the cavity contains new ceramic rings that provide an optimized absorption profile of electromagnetic radiation. This improved design TH1507U is a prototype of the 1.5-MW class CW Thales gyrotrons.

II. TH1507U Gyrotron at the W7-X Test Stand

In April 2024, the gyrotron was delivered to IPP Greifswald, Germany, and installed in the position D5 of the ECRH facility (Fig. 1). This position provides connection to a power supply allowing CW operation at cathode currents, I_c, of up to 100 A. The gyrotron is ran with a single-stage depressed collector. The applied scheme involves negative cathode voltages, U_c, a positive potential at the cavity (body voltage U_b), and the

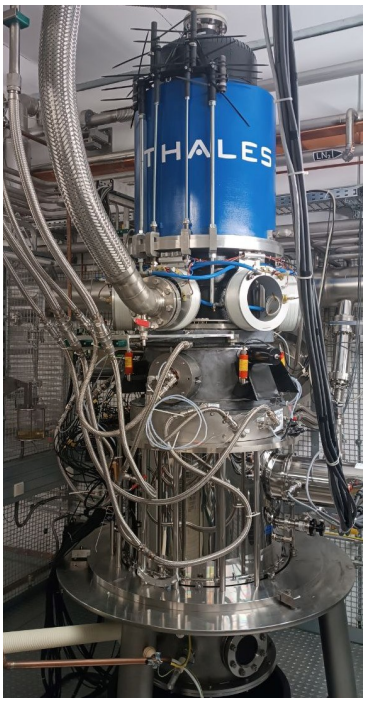

Fig. 1. Photograph of the novel 1.5-MW-class 140-GHz CW TH1507U gyrotron on the test stand at IPP Greifswald.

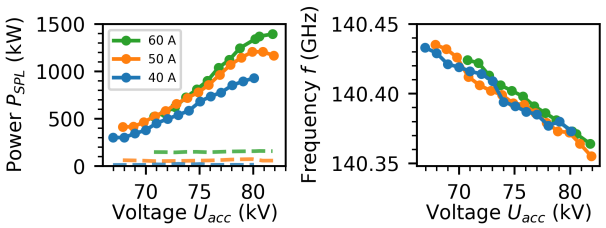

Fig. 2. Power P_{SPL} of the operating $TE_{28,10}$ mode measured in the short-pulse load (left, solid) and the corresponding frequency f (right) vs. accelerating voltage U_{acc} at various cathode currents I_c. The 1-ms body voltage U_b pulse is positioned in the middle of the 3-ms cathode voltage U_c pulse. The power radiated by the gyrotron at times outside the duration of the U_b pulse (left, dashed): 15 kW (I_c = 40 A), 60 kW (I_c = 50 A), 150 kW (I_c = 60 A).

TABLE I
LOW-CURRENT (LC) OPERATION IN THE $TE_{28,10}$ MODE

U_{acc}, kV	U_c, kV	I_c, A	P_{LPL}, kW	f, GHz (t=360 s)	δf, MHz (t_0=0.2 ms)	δf, MHz (t_0=1.5 ms)
66	41.5	40.6	194	140.396	90	37
70	44.4	40.9	355	140.299	179	121
74	48	41	566	140.217	251	183
77	52	40.4	737	140.162	299	225
80	54	40.2	930	140.123	328	250

collector at ground potential. The focusing magnetic field is created by a 5.6-T cryogen-free superconducting magnet (WO11660, Cryomagnetics, Inc.). The magnetic axis was adjusted in advance to the geometric axis of the borehole with a tolerance better than 0.1 mm.

The ECRH installation at W7-X includes a microwave quasi-optical transmission line (TL) operating under atmospheric pressure [9], [10]. The quasi-optical beams from the 12 gyrotron positions are guided in an underground beam duct to the W7-X experiment hall through large multi-beam mirrors in the form of two bundles of 6 beams each. During the commissioning phase, a gyrotron beam can be directed either to a short-pulse (<100 ms) load (SPL) or to a long-pulse calorimetric load (LPL), designed to operate with microwave beams of up to 2 MW. Both loads operate on the same principle. The focused beam is radiated through a small aperture and then fanned out by a conical reflector. The power is then absorbed by water flowing through Teflon pipes on the walls of the loads. For long-pulse operation, the beam polarization is set to circular in order to get isotropic power deposition on the load surface. The absorbed power readings, P_{LPL} or P_{SPL}, are determined calorimetrically by measuring the flow rate and temperature increase of the cooling water.

To search for the nominal mode, we conducted pulse tests with a length of τ = 0.5 ms and cathode currents $I_c \leq 40$ A, monitoring the shape of the gyrotron radiation at the output window and measuring its frequency. Thermal footprints of the microwave radiation were captured by using an infrared camera (FLIR Boson^{TM}) at a thin PVC target placed on the window flange. The frequency measurements are performed by using a highly sensitive heterodyne receiver from the collective Thomson scattering (CTS) diagnostic [11]. The CTS receiver shares the TL with the ECRH gyrotrons and collects stray radiation appearing in the duct due to diffraction of the gyrotron beam at the edges of the mirrors. The adjustment of the generated beam to the center of the diamond disk was performed after the nominal mode was detected. In addition, the pulse length was extended to 3 ms. The $TE_{28,10}$ mode is excited at accelerating voltages U_{acc} ranging from 66 kV to 80 kV and magnetic field configurations determined by the currents of the main coils I_m and gun coils I_g, which vary from 85 A to 86 A and from 2.5 A to 3.6 A, respectively. The corresponding magnetic field in the resonator ranges from 5.49 T to 5.53 T, while the pitch factor lies between 1.1 and 1.35. At I_c = 60 A, the gyrotron achieves 1.41 MW in the SPL load (Fig. 2) and up to 1.48 MW output power on the window.

Further commissioning of the tube enabled switching to the long-pulse operation and increased the pulse length τ to 360 s. The optimal operating parameters defined for I_c = 40 A are summarized in Table I. The gyrotron demonstrated an acceptable frequency shift $\delta f < 350$ MHz that was determined from the difference of frequencies measured at the end of the 360-s pulse and at $t = t_0$ from the beginning of the body voltage U_b pulse. The initial part of the time-frequency responses ($t < 20$ ms) is characterized by rapid frequency changes, related to neutralization processes in the tube. For instance, by operating the gyrotron at U_{acc} = 77 kV and I_c = 40 A (P_{LPL} = 737 kW), the frequency is f = 140.346 GHz at t_0 = 20 ms. Thus, the shift δf occurring due to the thermal expansion of the cavity is significantly lower. The indicated values were confirmed by separate measurements using a Frequency-Time Analyzer (FTA), which counts the 200 MHz clock cycles between the positive edges of a signal. The FTA is a part of the forward beam monitoring system, which is used to track the gyrotron power and frequency during plasma experiments. A small amount of gyrotron radiation is directed to the horn antenna of the analyzer by a fine grid placed on the first mirror of the TL.

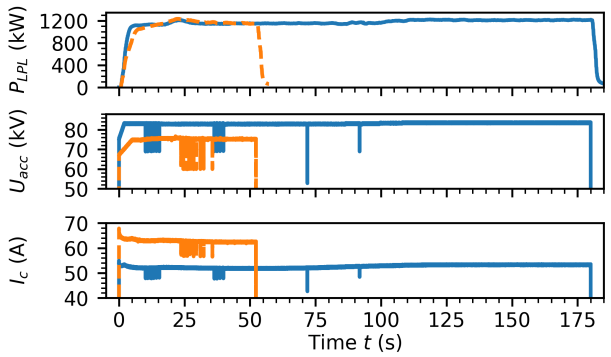

Fig. 3. Operation at the high-power regimes: (solid) a high-voltage, low-current regime ($U_{acc} = 83.5$ kV, $I_c = 53$ A, $I_m = 85.8$ A $I_g = 3.5$ A); (dashed) a low-voltage, high-current regime ($U_{acc} = 75$ kV, $I_c = 62.4$ A, $I_m = 84.65$ A $I_g = 2.5$ A). Narrow negative spikes in the accelerating voltage and cathode current time traces indicate the activation of the mode recovery system [14], which triggers when the nominal mode is lost. The system ramps down the U_{acc} voltage to excite the nominal mode at lower power and then increases the voltage to the operating value. The mode typically recovers within 1 ms.

TABLE II
OPERATING REGIMES OF TH1507U GYROTRON IN THE $TE_{28,10}$ MODE

Parameter	LC	HVLC	LVHC
Accelerating voltage, U_{acc} (kV)	79	83.5	75
Cathode current, I_c (A)	40	53.2	62.4
Current of main coils, I_m (A)	85.65	85.8	84.7
Current of gun coils, I_g (A)	2.8	3.5	2.5
Frequency, f (GHz)	140.136	140.098	140.119
Measured power, P_{LPL} (kW)	897	1216	1152
Output Power, P_{out} (kW)	964	1309	1239
Total efficiency (%)	46.6	45.9	40.4
Calorimetric Power Dissipation Measurements (kW)			
Collector, $P_{coll.}$	964	1212	1518
Cavity and M1, $P_{cav.}$	30	37	34
Launcher, M1 and M2, $P_{lnch.}$	10.5	15.5	11
Inner load and M3, P_{IL}	2.5	3.8	3.9
Mirror box and relief load, $P_{MB} + P_{RL}$	3.6	6.9	7.6
Output and relief load windows	1.6	1.8	1.7

The consistent increase of the I_c and optimization of the transverse field sweeping system [12], [13] by monitoring the temperature distribution in the collector brought the gyrotron into operation at currents I_c from 50 A to 65 A. The tests for maximum power defined two possible regimes (Fig. 3): the nominal regime with high accelerating voltage and low current (HVLC) and the low-voltage, high-current regime (LVHC).

Table II summarizes the parameters of the gyrotron for the related pulses. The output power P_{out} of the gyrotron is derived from the measurements and the power lost in the TL. There are 5 mirrors and 2 polarizers between the LPL and the gyrotron. The accounted transmission losses include ohmic losses in the mirrors, truncation of the Gaussian beam, power reflected by the load and atmospheric absorption of microwaves. Both high-power operating regimes demonstrated a saturation of power P_{out} at 1.2-1.3 MW that is accompanied by an increase in the dissipated power on the internal gyrotron components. This power is monitored calorimetrically through the corresponding cooling circuits. The losses in the mirror box P_{MB} and in the relief load P_{RL} prevail (Fig. 4), which at $I_c > 50$ A are double with respect to the low-current (LC) regime. The search for possible parasitic modes in the range

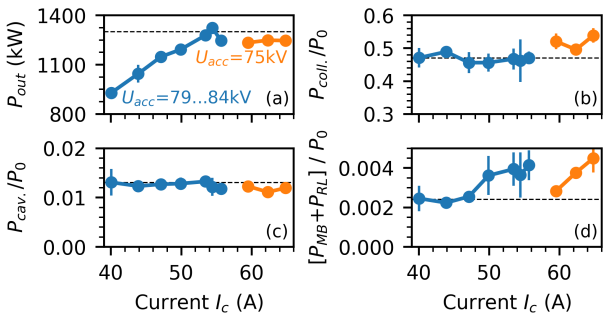

Fig. 4. (a) Optimal output power and corresponding dissipated power (b) in the collector $P_{coll.}$, (c) in the cavity $P_{cav.}$, (d) in the mirror box and relief load $P_{MB} + P_{RL}$ vs. the cathode current. Dissipated power is normalized by the input beam power P_0.

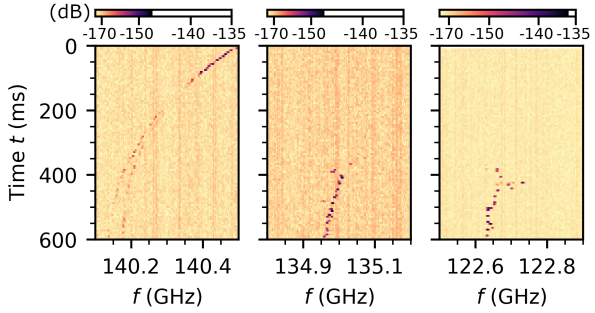

Fig. 5. Spectrograms recorded by the fast ADC of the CTS receiver when the gyrotron power P_{LPL} is modulation between 600 kW and 1100 kW at 50 Hz ($U_{acc} = 76.5$ - 85 kV, $I_c = 52$ - 58 A, $I_m = 86$ A, $I_g = 3.6$ A). The parasitic modes (middle, right) were detected only at the high-power sections. The receiver contains a notch filter that attenuates signals by more than 100 dB in the range from 140.0 GHz to 140.3 GHz.

from 120.9 GHz to 142.1 GHz demonstrated excitation at 134.9 GHz and at 122.6 GHz (Fig. 5). Both parasitic modes show pronounced spectral lines at $I_c > 55$ A. However, the power spectral density of the 134.9-GHz mode is rather weak compared to the second one, which, in the relief load, has the same order of magnitude as the nominal $TE_{28,10}$ mode.

III. CONCLUSION

The first long-pulse experiments with the 1.5-MW 140-GHz CW TH1507U prototype gyrotron demonstrated efficient operation at the nominal cavity mode. The maximal output power of up to 1.3 MW was achieved in the HVLC regime with a total efficiency of 45.9% with depressed collector. The CW operation was demonstrated for a pulse length of up to 580 s and an output power of 1.2 MW ($U_{acc} = 83$ kV, $I_c = 46.5$ A, $I_m = 86$ A $I_g = 3.6$ A). Output power saturation was noticed at 1.3 MW, which can be explained by the rise of parasitic waves in the cavity and/or the beam tunnel, as was already observed in earlier series of the TH1507 gyrotron [15]. This effect will be investigated further. Nevertheless, the developed oscillator has already demonstrated outstanding experimental performance compared to existing gyrotrons operating with pulse durations exceeding 100 seconds [16], [17], [18].

ACKNOWLEDGMENT

Views and opinions expressed are however those of the authors only and do not necessarily reflect those of the European Union or the European Commission. Neither the European Union nor the European Commission can be held responsible for them.

REFERENCES

[1] R. C. Wolf, C. D. Beidler, A. Dinklage, P. Helander, H. P. Laqua, F. Schauer, T. S. Pedersen, and F. Warmer, "Wendelstein 7-X program—Demonstration of a stellarator option for fusion energy," *IEEE Trans. Plasma Sci.*, vol. 44, no. 9, pp. 1466–1471, Sep. 2016, doi: 10.1109/TPS.2016.2564919.

[2] H. P. Laqua, K. A. Avramidis, H. Braune, I. Chelis, G. Gantenbein, S. Illy, Z. Ioannidis, J. Jelonnek, J. Jin, L. Krier, C. Lechte, A. Leggieri, F. Legrand, S. Marsen, D. Moseev, H. Oosterbeek, T. Rzesnicki, T. Ruess, T. Stange, M. Thumm, I. Tigelis, and R. C. Wolf, "The ECRH-power upgrade at the wendelstein 7-X stellarator," in *Proc. EPJ Web Conf.*, vol. 277, Feb. 2023, p. 04003, doi: 10.1051/epjconf/202327704003.

[3] K. A. Avramidis, T. Ruess, F. Mentgen, J. Jin, D. Wagner, G. Gantenbein, S. Illy, C. Ioannidis, H. P. Laqua, I. G. Pagonakis, T. Rzesnicki, M. Thumm, R. C. Wolf, and J. Jelonnek, "Studies towards an upgraded 1.5 MW gyrotron for W7-X," in *Proc. EPJ Web Conf.*, vol. 203, Mar. 2019, p. 4003, doi: 10.1051/epjconf/201920304003.

[4] K. A. Avramidis, Z. C. Ioannidis, G. Aiello, P. Bénin, I. Chelis, A. Dinklage, G. Gantenbein, S. Illy, J. Jelonnek, J. Jin, H. P. Laqua, A. Leggieri, F. Legrand, A. Marek, S. Marsen, I. G. Pagonakis, T. Ruess, T. Rzesnicki, T. Scherer, D. Strauss, M. Thumm, I. Tigelis, D. Wagner, J. Weggen, and R. C. Wolf, "Towards a 1.5 MW, 140 GHz gyrotron for the upgraded ECRH system at W7-X," *Fusion Eng. Des.*, vol. 164, Mar. 2021, Art. no. 112173, doi: 10.1016/j.fusengdes.2020.112173.

[5] Z. C. Ioannidis, K. A. Avramidis, T. Rzesnicki, I. Chelis, G. Gantenbein, S. Illy, J. Jin, I. Gr. Pagonakis, M. Thumm, and J. Jelonnek, "Generation of 1.5 MW–140 GHz pulses with the modular pre-prototype gyrotron for W7-X," *IEEE Electron Device Lett.*, vol. 42, no. 6, pp. 939–942, Jun. 2021, doi: 10.1109/LED.2021.3073221.

[6] K. A. Avramidis, Z. C. Ioannidis, S. Illy, J. Jin, T. Ruess, G. Aiello, M. Thumm, and J. Jelonnek, "Multifaceted simulations reproducing experimental results from the 1.5-MW 140-GHz preprototype gyrotron for W7-X," *IEEE Trans. Electron Devices*, vol. 68, no. 6, pp. 3063–3069, Jun. 2021, doi: 10.1109/TED.2021.3075653.

[7] G. Dammertz, S. Alberti, A. Arnold, E. Borie, V. Erckmann, G. Gantenbein, E. Giguet, R. Heidinger, J. P. Hogge, S. Illy, W. Kasparek, K. Koppenburg, M. Kuntze, H. P. Laqua, G. LeCloarec, Y. LeGoff, W. Leonhardt, C. Lievin, R. Magne, G. Michel, G. Muller, G. Neffe, B. Piosczyk, M. Schmid, K. Schworer, M. K. Thumm, and M. Q. Tran, "Development of a 140-GHz 1-MW continuous wave gyrotron for the W7-X stellarator," *IEEE Trans. Plasma Sci.*, vol. 30, no. 3, pp. 808–818, Jun. 2002, doi: 10.1109/TPS.2002.801509.

[8] A. Leggieri, S. Alberti, K. A. Avramidis, G. Dammertz, V. Erckmann, G. Gantenbein, J.-P. Hogge, S. Illy, Z. Ioannidis, J. Jelonnek, J. Jin, H. Laqua, F. Legrand, C. Lievin, R. Marchesin, I. G. Pagonakis, T. Rzesnicki, P. Thouvenin, M. Thumm, and R. Wolf, "THALES TH1507 140 GHz 1 MW CW gyrotron for W7-X stellarator," in *Proc. 44th Int. Conf. Infr., Millim., THz Waves (IRMMW-THz)*, Paris, France, Sep. 2019, pp. 1–3, doi: 10.1109/IRMMW-THz.2019.8874589.

[9] V. Erckmann, P. Brand, H. Braune, G. Dammertz, G. Gantenbein, W. Kasparek, H. P. Laqua, H. Maassberg, N. B. Marushchenko, G. Michel, M. Thumm, Y. Turkin, M. Weissgerber, and A. Weller, "Electron cyclotron heating for W7-X: Physics and technology," *Fusion Sci. Technol.*, vol. 52, no. 2, pp. 291–312, Aug. 2007, doi: 10.13182/fst07-a1508.

[10] V. Erckmann, W. Kasparek, G. Gantenbein, F. Hollmann, L. Jonitz, F. Noke, F. Purps, and M. Weissgerber, "ECRH for W7-X: Transmission losses of high-power 140-GHz wave beams," *Fusion Sci. Technol.*, vol. 55, no. 1, pp. 16–22, Jan. 2009, doi: 10.13182/fst09-a4049.

[11] S. Ponomarenko, D. Moseev, T. Stange, L. Krier, P. Stordiau, H. Braune, G. Gantenbein, J. Jelonnek, A. Kuleshov, H. P. Laqua, C. Lechte, S. Marsen, S. K. Nielsen, J. W. Oosterbeek, B. Plaum, R. Ragona, J. Rasmussen, T. Ruess, M. Salewski, M. Thumm, J. Zimmermann, and W.-X. Team, "Development of the 174 GHz collective Thomson scattering diagnostics at Wendelstein 7-X," *Rev. Sci. Instrum.*, vol. 95, no. 1, Jan. 2024, Art. no. 013501, doi: 10.1063/5.0174444.

[12] M. Schmid, S. Illy, G. Dammertz, V. Erckmann, and M. Thumm, "Transverse field collector sweep system for high power CW gyrotrons," *Fusion Eng. Des.*, vol. 82, nos. 5–14, pp. 744–750, Oct. 2007, doi: 10.1016/j.fusengdes.2007.06.008.

[13] H. Braune, V. Erckmann, S. Illy, H. P. Laqua, G. Michel, F. Noke, and F. Purps, "Transverse field collector sweeping for the W7-X gyrotrons-modulation techniques," in *Proc. IRMMW*, Busan, South Korea, Nov. 2009, pp. 1–2, doi: 10.1109/ICIMW.2009.5325739.

[14] F. Wilde, S. Marsen, T. Stange, D. Moseev, J. W. Oosterbeek, H. P. Laqua, R. C. Wolf, K. Avramidis, G. Gantenbein, I. G. Pagonakis, S. Illy, J. Jelonnek, and M. K. Thumm, "Automated mode recovery for gyrotrons demonstrated at Wendelstein 7-X," *Fusion Eng. Des.*, vol. 148, Nov. 2019, Art. no. 111258, doi: 10.1016/j.fusengdes.2019.111258.

[15] G. Gantenbein, V. Erckmann, S. Illy, S. Kern, W. Kasparek, C. Lechte, W. Leonhardt, C. Liévin, A. Samartsev, A. Schlaich, M. Schmid, and M. Thumm, "140 GHz, 1 MW CW gyrotron development for fusion applications—Progress and recent results," *J. Infr., Millim., THz Waves*, vol. 32, no. 3, pp. 320–328, Mar. 2011, doi: 10.1007/s10762-010-9749-2.

[16] A. G. Litvak, G. G. Denisov, and M. Y. Glyavin, "Russian gyrotrons: Achievements and trends," *IEEE J. Microw.*, vol. 1, no. 1, pp. 260–268, Jan. 2021, doi: 10.1109/JMW.2020.3030917.

[17] A. G. Litvak, G. G. Denisov, A. G. Eremeev, M. Yu. Glyavin, E. A. Kopelovich, L. G. Popov, A. N. Kuftin, E. V. Sokolov, E. A. Soluyanova, E. M. Tai, A. I. Tsvetkov, and V. E. Zapevalov, "The progress in the development of gyrotrons for plasma installations in Russia," in *Proc. IRMMW-THz*, Buffalo, NY, USA, Nov. 2020, p. 1, doi: 10.1109/IRMMW-THz46771.2020.9370526.

[18] M. Thumm, "State-of-the-art of high-power gyro-devices and free electron masers," *J. Infr., Millim., THz Waves*, vol. 41, pp. 1–140, Jan. 2020, doi: 10.1007/s10762-019-00631-y.